ACS Macro Letters

Letter

pubs.acs.org/macroletters

Shape Memory Assisted Self-Healing Coating

Xiaofan Luo† and Patrick T. Mather*

Department of Biomedical and Chemical Engineering, Syracuse Biomaterials Institute, Syracuse, New York 13244, United States

Supporting Information

ABSTRACT: In this communication, we report the preparation and characterization of new shape memory assisted self-healing (SMASH) coatings. The coatings feature a phase-separated morphology with electrospun thermoplastic poly(ε-caprolactone) (PCL) fibers randomly distributed in a shape memory epoxy matrix. Mechanical damage to the coating can be self-healed via heating, which simultaneously triggers two events: (1) the shape recovery of the matrix to bring the crack surfaces in spatial proximity, and (2) the melting and flow of the PCL fibers to rebond the crack. In controlled healing experiments, damaged coatings not only heal structurally, but also functionally by almost completely restoring the corrosion resistance. We envision the wide applicability of the SMASH concept in designing the next-generation self-healing materials.

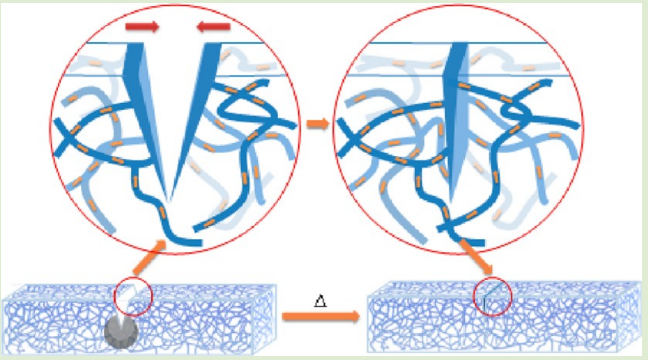

Metallic corrosion has long been a major problem for industries in the U.S. and worldwide. According to a landmark study conducted by Battelle Memorial Institute and the Specialty Steel Industry of North America, the annual cost of corrosion in the U.S. was approximately $442 billion in 2007 or 3.1% of the Gross Domestic Product (GDP).[1] One of the major methods employed to prevent corrosion is to apply a "barrier" organic, usually a polymeric coating, on the metal surface. However, most polymeric coatings are susceptible to impairments induced by environmental degradation and mechanical damage, which, if not repaired properly, can lead to compromised corrosion resistance or even macroscopic failure of the coating. With conventional coating technologies, repair of a coating is tedious at best and often involves extensive labor as well as high cost. There has been a constant market demand for coating materials that can "self-heal", that is, possessing an intrinsic ability to heal damage with no or minimum external intervention.

The field of self-healing polymers has attracted a significant amount of research efforts during the past decade.[2,3] Self-healing is increasingly becoming an important concept in the design of polymeric materials and composites. Broadly speaking, three major strategies have been established to incorporate self-healing functionality to polymer systems: (1) damage-initiated in situ polymerization of monomeric "healing agents",[4,5] (2) reversible chemistry based reconstruction of the molecular network,[6] and (3) incorporation of fusible thermoplastics in a thermoset host.[7,8] At least two of these approaches have also been implemented in coatings. For example, Cho et al.[9] and Park and Braun[10] reported self-healing coatings with liquid, reactive healing agents hosted in microcapsules and core/sheath fibers, respectively. Using the reversible Diels–Alder reaction, Wouters et al.[11] developed thermoset coatings that can be self-healed via a thermal treatment, although the healing process involved a complete liquification of the coating material.

Over the last several years, a new concept has emerged that explores the use of shape memory materials to improve the self-healing process by providing a mechanism to partially or fully close the crack. This concept, which we term shape memory assisted self-healing (SMASH), has been demonstrated in at least two approaches. The first approach utilizes pretensioned shape memory alloy (SMA) wires[12−14] or shape memory polymer (SMP) fibers[15,16] that, when activated, exert a contractual force that pulls the crack surfaces closer. An apparent shortcoming in this approach is the fact that the SMA wires or SMP fibers have to be positioned locally and perpendicular to the crack in order to be effective, which is challenging to achieve in practical applications. The second SMASH approach utilizes "bulk" shape memory from the material to close the crack.[17,18] One example is the poly(ε-caprolactone) (PCL) based molecular composite system recently reported by our group.[17] That particular material was a single-phase, two-component blend composed of a thiol−ene cross-linked PCL network (n-PCL) and a high M_w linear PCL (l-PCL) interpenetrating the network. The n-PCL exhibits "reversible plasticity", a form of shape memory where large plastic deformation at room temperature (*below* the shape memory transition temperature) is fully recoverable upon heating. This shape memory from n-PCL assists in closing any cracks and damage, whereas the mobile l-PCL chains (the self-healing agent in this case) tackify the crack surfaces via diffusion

Received: January 14, 2013
Accepted: January 28, 2013
Published: February 1, 2013

   dx.doi.org/10.1021/mz400017x | *ACS Macro Lett.* 2013, 2, 152−156

and ultimately rebond the crack to restore mechanical strength. Both crack closure and rebonding are achieved by a single heating step with no additional intervention.

In this communication, we introduce a new SMASH strategy detailing the preparation of a new self-healing material tailored for coating/corrosion-inhibition applications. Unlike the single-phase n-PCL/l-PCL system, the coatings exhibit a phase-separated morphology wherein the thermoplastic healing agent exists as randomly oriented, nonwoven nano- and microfibers evenly distributed in a shape memory thermoset matrix. Conceptually, this morphology enables more significant flow of the liquefied thermoplastic compared to the limited diffusion distance in the case of a miscible, single-phase blend, therefore, allowing the healing of larger cracks and defects. Yet the high aspect ratio fibers are more efficient than many other geometries (such as spheres) in creating a large interfacial area and providing more sustained healing agent delivery.

The overall concept is further illustrated in Figure 1. Typical damage to a polymeric coating usually contains two forms:

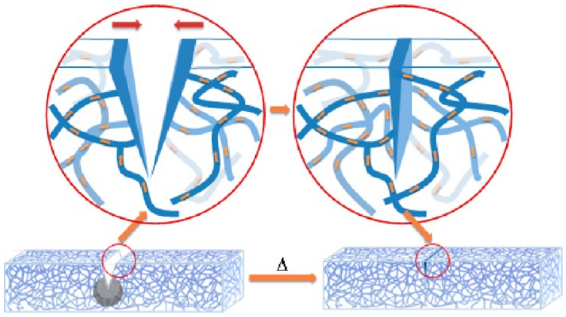

Figure 1. Schematic illustration of the coating morphology and the shape memory assisted self-healing (SMASH) concept.

plastic/permanent deformation, indicated as the shaded area surrounding the crack tip, and cracks involving the creation of free surfaces. In severe cases, some portions of the material may even be permanently removed from the coating, leaving voided space. Self-healing is initiated by heating the damaged coating to a temperature higher than both the liquefying temperature of the fibers (in this case, melting temperature or T_m) as well as the transition temperature (glass transition temperature or T_g) of the SMP matrix. Two events take place simultaneously: (1) recovery of the SMP matrix that releases the stored strain energy in the plastic zone and closes the crack, that is, bringing crack surfaces into spatial proximity, and (2) melting and flow of the thermoplastic to rebond the crack. The most significant advantage of SMASH is that the crack closure minimizes the healing agent needed. Therefore, healing of large cracks and voids becomes possible.

The new self-healing coating was prepared via a two-step process. The first step involved direct solution electrospinning of PCL (T_m ca. 60 °C) onto a steel substrate (3 × 3 cm) using the setup shown in Figure 2A,B (more details in Experimental Methods). This led to a uniform, fibrous coating on the steel substrate, as shown by the photograph in Figure 2C. The SEM image (Figure 2E) reveals a structure of continuous PCL fibers that are randomly oriented, with an average fiber diameter (measured by image analysis) of 1.38 ± 0.87 μm. In the second step, a shape memory epoxy formulation[19] consisting of an equimolar mixture of diepoxide, diglycidyl ether of bisphenol A (DGEBA), neopentyl glycol diglycidyl ether (NGDE), and poly(propylene glycol)bis(2-amino- propyl) ether (Jeffamine

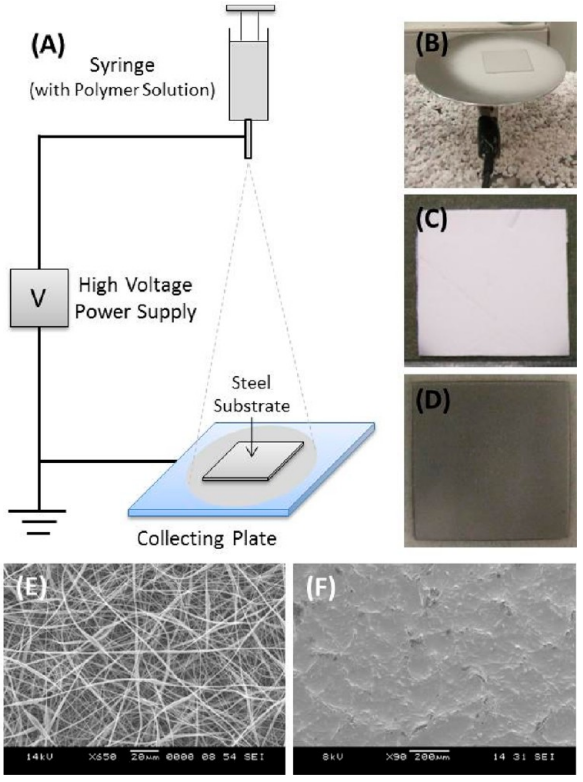

Figure 2. Process to prepare the SMASH coatings. (A) Schematic illustration of the electrospinning setup; (B) photograph showing the actual electrospinning process; (C) PCL-coated steel substrate after electrospinning for 10 min; (D) steel substrate after spin-coating of epoxy, (E) SEM image of the PCL-coated surface, and (F) SEM image of the final coating.

D230) was spin-coated onto the PCL-coated steel substrate. The liquid epoxy could easily wet the PCL fibers due to favorable surface energetics but does not lead to any dissolution or swelling of PCL (this has been thoroughly studied in our previous publication[20]). One advantage of the spin-coating technique is the automatic removal of the excess epoxy by the centrifugal force from high-speed spinning. The epoxy-coated specimens were allowed to fully cure first at room temperature for 72 h and then at 40 °C for 24 h. This particular epoxy formulation led to a glassy SMP with a T_g of about 50 °C.[21] After curing, a translucent, void-free and rigid coating was formed on the steel substrate (Figure 2D,F). The average PCL weight fraction in the final coatings was measured gravimetrically to be about 12%.

One important structural variable in the current self-healing coating system (or any self-healing coatings) is the coating thickness, mainly because it determines the amount of healing agent available for damage of a given size. In our case, the coating thickness can be controlled simply by the electrospinning time. As discussed above, PCL acts essentially as a "primer" that retains the necessary amount of epoxy to form a continuous matrix, while any excess amount of epoxy is removed by spinning. Therefore the total coating (epoxy/PCL) thickness is dictated only by the fiber (PCL) layer thickness, which in turn can be controlled (other conditions remaining the same) by the time of electrospinning. This was confirmed by measuring final coating thicknesses of various electrospinning times. As shown in Figure 3, the coating thickness

dx.doi.org/10.1021/mz400017x | ACS Macro Lett. 2013, 2, 152−156

increases linearly with electrospinning time, with a slope of 11 μm/min.

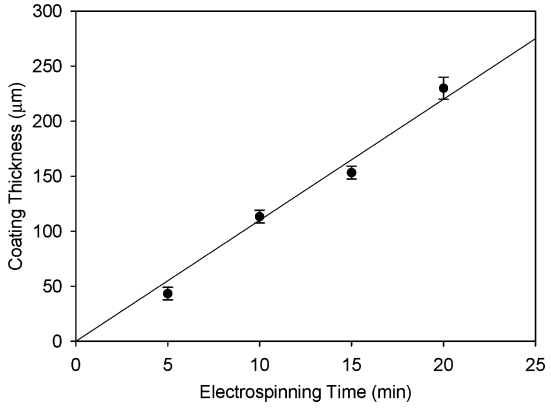

Figure 3. Final epoxy/PCL coating thickness plotted as a function of PCL electrospinning time, showing facile control of coating thickness via the latter.

The self-healing capability of the prepared epoxy/PCL coatings was first visualized using optical microscopy (Figure 4). For this experiment, three methods were used to introduce damage of various degrees. In the first case (Figure 4A), the coating was scratched using a blunt geometry (a spatula with d = 1 mm), which led to primarily plastic deformation (no crack formation). The scratched coating was then heated on a hot-stage at 2 °C/min to 80 °C, with the damaged site continuously imaged using a stereo microscope and a CCD camera. As observed, this heating completely recovers the plastic deformation and heals the scratch. In this scenario, only shape memory (or more specifically, reversible plasticity shape memory) was utilized because no crack was formed. It also agrees with recent reports that reversible plasticity shape memory not only exists in semicrystalline but also in glassy SMPs.[22] The second damaging method involved the use of a fresh razor blade (Figure 4B), which created a relatively "clean" crack as well as plastic deformation that separated the crack surfaces. The most severe damage was created by using a conical scribe (Figure 4C; more details on the damaging methods available in Supporting Information). In this case, the circular contact between the scribe and the coating led to a severe stress state with small cracks randomly propagating around the main damaging path (more clear in Figure 5C). There was also some permanent material loss, although not quantified. For both damage scenarios, a simple heating step (2 °C/min to 80 °C) resulted in significant closure of the damage

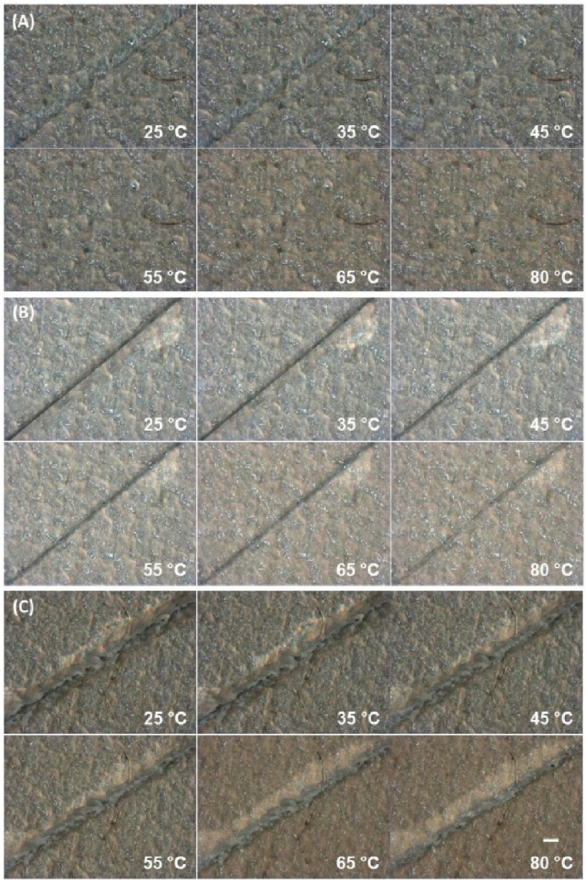

Figure 4. Stereo-optical micrographs showing the self-healing of coatings damaged by a (A) blunt spatula, (B) razor blade, and (C) conical scribe. The damaged coating was heated from 25 to 80 °C at 2 °C/min. The scale bar (bottom right) represents 200 μm. Continuous movies are available in Supporting Information.

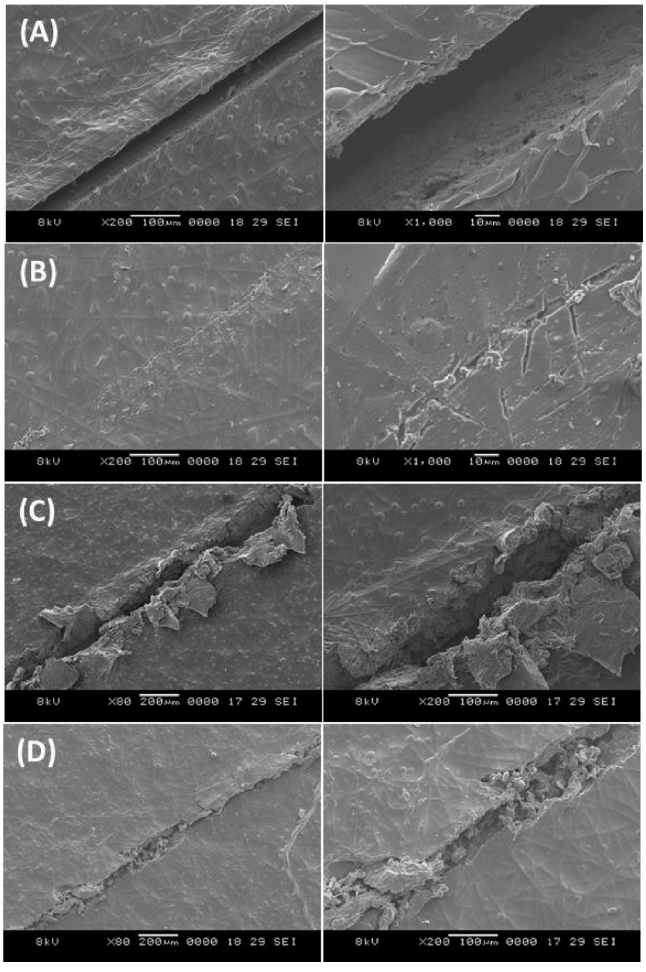

Figure 5. Scanning electron micrographs of a (A) cracked coating, (B) crack coating after self-healing, (C) scribed coating, and (D) scribed coating after self-healing. The self-healing was conducted by heating at 80 °C for 10 min.

dx.doi.org/10.1021/mz400017x | ACS Macro Lett. 2013, 2, 152−156

bringing crack surfaces close to each other. Movies of the self-healing processes are available in Supporting Information.

Scanning electron microscopy (SEM) was utilized to further examine the crack closure at higher magnification. Figure 5 compares the damaged site before and after self-healing for both "cracked" and "scribed" coatings. As shown in Figure 5A, the original crack gap (distance between the crack surfaces) was about 50 μm. After self-healing (heating at 80 °C for 10 min), the crack was completely closed, with almost no detectable separation. Similar crack closure was observed for the scribed coating (Figure 5B), although some voids (due to permanent material loss) are still visible.

The results presented so far have revealed encouraging structural self-healing of the epoxy/PCL coatings. This effectively brings the separated crack surfaces in spatial proximity to facilitate crack rebonding by the molten PCL. Such crack rebonding is difficult to "visualize" (partly because of the closed crack), but can be characterized from the functional self-healing, that is, the restoration of corrosion resistance in self-healed coatings. If the crack surfaces are closed but not rebonded, corrosive agents such as water and oxygen can still penetrate through the coating and induce corrosion. In other words, only when the cracks are both closed and rebonded can corrosion resistance (the barrier function of the coating) be reasonably restored.

The corrosion resistance was characterized electrochemically via linear sweep voltammetry using a three-electrode setup (more details in Experimental Methods and Supporting Information). Fully cured epoxy/PCL coatings were damaged using the razor blade method. Care was taken to ensure that the cracks penetrated the entire coating thickness. Coatings prepared under two different electrospinning times, 10 min (thickness of ca. 110 um) and 15 min (thickness of ca. 155 um), were tested. The voltage (V) versus current (I) results are presented in Figure 6A. A significant difference was observed between the damaged/cracked and self-healed coatings. For both 10 min and 15 min electrospun coatings that were damaged, relatively large electrical currents were detected, indicating active corrosion of the exposed area on the steel substrate. Visual examination of the specimens after the experiment reveals clear formation of rust around the damage (Figure 6B,C). In contrast, very little electrical current was detected for the self-healed specimens (Figure 6A) and no rust formation can be visually observed (Figure 6B,C). In fact, the electrical current of 15 min electrospun coating was below the detection limit of the potentiostat (10^{-6} mA), and the obtained data was primarily instrumental noise. This indicates effective, functional self-healing, that is, complete restoration of the barrier function. Microscopic examination of the damaged site also shows complete crack closure and self-healing due to SMASH mechanism (Figure S6 in Supporting Information). The restored corrosion resistance was further confirmed in a long-term, salt water immersion experiment in which self-healed coatings exhibited considerably less corrosion creepage around the damage (Supporting Information).

To conclude, this communication has introduced the design and preparation methods of a new self-healing coating featuring a SMASH mechanism. Excellent self-healing performance has been demonstrated from almost completely restored barrier function/corrosion resistance. There are many potential directions to further develop this material system. For example, one may incorporate corrosion inhibitors[23] in the fibers, which can be released during the same self-healing process to further minimize corrosion, or one can utilize magnetic fillers in the shape memory matrix to achieve remotely activated self-healing.[24,25] We envision broad applicability of the SMASH concept in the designing of next-generation self-healing materials.

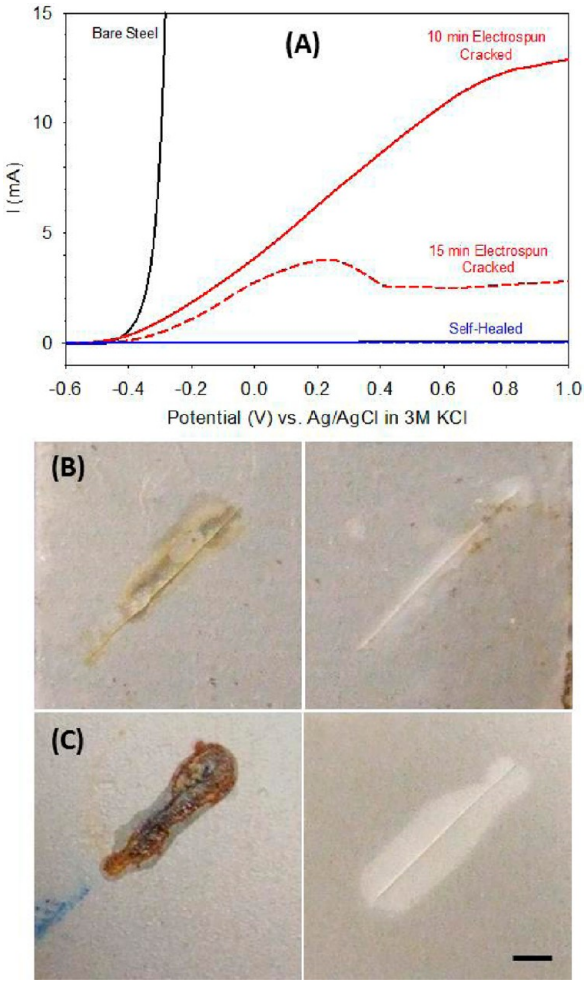

Figure 6. Linear sweep voltammetry experiment. (A) I vs V plots for bare steel (control), two damaged coatings (with different thicknesses), and self-healed coatings. The photos of the exposed areas of damaged and self-healed coatings after the linear sweep voltammetry testing are also shown: (B) 10 min and (C) 15 min electrospun. The scale bar (bottom right) represents 2 mm.

EXPERIMENTAL METHODS

Materials: All materials, including poly(ε-caprolactone) (PCL, M_w = 65000 g/mol), poly(diglycidyl ether of bisphenol A (DGEBA), neopentyl glycol diglycidyl ether (NGDE), and poly(propylene glycol)bis(2-amino-propyl) ether (Jeffamine D230) were purchased from Sigma-Aldrich and used as received.

Coating Preparation: PCL was first electrospun directly onto a 3 × 3 cm steel substrate (general purpose 1074/1075 spring steel from McMaster-Carr) from a solution (2 g of PCL dissolved in 8 mL of chloroform and 2 mL of DMF), using the setup shown in Figure 2. The electrospinning parameters are as follows: flow rate = 1 mL/h, voltage = 12 kV, and top-to-collector distance = 15 cm. To introduce the epoxy matrix, equimolar DGEBA (preheated at 70−80 °C to melt the crystals formed during storage), NGDE, and Jeffamine D230 were mixed and hand-stirred at r.t. until a clear, homogeneous, and low-viscosity mixture was obtained. The mixture was then spin-coated on PCL-coated steel panels using a Laurell WS-400B-6NPP/Lite spin processor. The spin program was set as follows: (1) 300 rpm for 10 s;

dx.doi.org/10.1021/mz400017x | ACS Macro Lett. 2013, 2, 152−156

during this low-speed step, 1−1.5 mL of epoxy mixture was dispensed dropwise through the attached syringe; (2) 1000 rpm for 20 s; (3) 2000 rpm for 20 s; and finally, (4) 3000 rpm for 20 s. The coatings were finally cured at r.t. for 72 h and then at 40 °C for 24 h.

Coating Damaging Methods: A coated steel panel (3 × 3 cm) was fixed to a square set using a parallel clamp. The damage was introduced along the diagonal by scratching the coating with either a spatula, a fresh razor blade, or a cone-shaped carbide scribe (McMaster-Carr, Catalog # 2157A11) to produce different types of damage (see discussions in the main text).

Microscopy: To monitor the damaged area during self-healing, a damaged coating sample was placed on an Instec HCS-402 hot-stage and heated from 25 to 80 °C at a constant heating rate of 2 °C/min. A Zeiss Discovery V8 stereo microscope equipped with a QImaging CCD camera was used to capture digital images at a rate of 2 frames/s. A JEOL JSM5600 scanning electron microscope was used to further examine the damage before and after self-healing. A typical accelerating voltage of 10 kV was used for SEM.

Linear Sweep Voltammetry: A three-electrode setup with an electrochemical cell specifically designed for plate geometries (plate material evaluating cell purchased from Bio-Logic Science Instruments) and a Bio-Logic SP-50 potentiostat were used for the experiments. The coating specimen was loaded onto the electrochemical cell with a portion of the damaged/self-healed area exposed to a 5 wt % NaCl/H_2O solution. The working, counter, and reference electrodes were the coating substrate, Pt, and Ag/AgCl in 3 M KCl solution, respectively. The open circuit potential (OCP) was first monitored until it became stable versus time. The voltage (relative to the reference electrode) was then linearly scanned from −0.8 to 1 V at a constant rate of 20 mV/s while recording the electrical current data. More details about the experimental setup are provided in the Supporting Information.

■ ASSOCIATED CONTENT

Supporting Information

(1) Schematic illustration of typical types of coating damage and the associated SMASH mechanisms, (2) schematic illustration of the coating damaging methods, (3) schematic illustration of the spin-coating process, (4) continuous movies showing the self-healing processes, (5) the detailed experimental setup for the linear sweep voltammetry experiment, (6) stereo-optical micrographs showing the crack healing of the specimens used in linear sweep voltammetry, and (7) salt-water immersion experiment. This material is available free of charge via the Internet at http://pubs.acs.org.

■ AUTHOR INFORMATION

Corresponding Author

*E-mail: ptmather@syr.edu.

Present Address

[†]Flow Polymers, LLC, 12819 Coit Rd., Cleveland, OH 44108.

Notes

The authors declare no competing financial interest.

■ ACKNOWLEDGMENTS

The authors would like to acknowledge Prof. Jeremy Gilbert at the Department of Biomedical and Chemical Engineering, Syracuse University, for his help with electrochemical measurements.

■ REFERENCES

(1) The Annual Cost of Corrosion to Ohio, http://www.brown.senate.gov/imo/media/doc/OhioCorrosion.pdf.

(2) Blaiszik, B. J.; Kramer, S. L. B.; Olugebefola, S. C.; Moore, J. S.; Sottos, N. R.; White, S. R. *Annu. Rev. Mater. Res.* **2010**, *40*, 179−211.

(3) Murphy, E. B.; Wudl, F. *Prog. Polym. Sci.* **2010**, *35*, 223−251.

(4) White, S. R.; Sottos, N. R.; Geubelle, P. H.; Moore, J. S.; Kessler, M. R.; Sriram, S. R.; Brown, E. N.; Viswanathan, S. *Nature* **2001**, *409*, 794−7.

(5) Trask, R. S.; Bond, I. P. *Smart Mater. Struct.* **2006**, *15*, 704−710.

(6) Chen, X.; Dam, M. a; Ono, K.; Mal, A.; Shen, H.; Nutt, S. R.; Sheran, K.; Wudl, F. *Science* **2002**, *295*, 1698−702.

(7) Luo, X.; Ou, R.; Eberly, D. E.; Singhal, A.; Viratyaporn, W.; Mather, P. T. *ACS Appl. Mater. Interfaces* **2009**, *1*, 612−620.

(8) Meure, S.; Wu, D. Y.; Furman, S. *Acta Mater.* **2009**, *57*, 4312−4320.

(9) Cho, S. H.; White, S. R.; Braun, P. V. *Adv. Mater.* **2009**, *21*, 645−649.

(10) Park, J.-H.; Braun, P. V. *Adv. Mater.* **2010**, *22*, 496−499.

(11) Wouters, M.; Craenmehr, E.; Tempelaars, K.; Fischer, H.; Stroeks, N.; Vanzanten, J. *Prog. Org. Coat.* **2009**, *64*, 156−162.

(12) Kirkby, E. L.; Rule, J. D.; Michaud, V. J.; Sottos, N. R.; White, S. R.; Månson, J.-A. E. *Adv. Funct. Mater.* **2008**, *18*, 2253−2260.

(13) Kirkby, E. L.; Michaud, V. J.; Månson, J. -a. E.; Sottos, N. R.; White, S. R. *Polymer* **2009**, *50*, 5533−5538.

(14) Neuser, S.; Michaud, V.; White, S. R. *Polymer* **2012**, *53*, 370−378.

(15) Li, G.; Meng, H.; Hu, J. *J. R. Soc. Interface* **2012**, *9*, 3279−87.

(16) Li, G.; Shojaei, a. *Proc. R. Soc. A* **2012**, *468*, 2319−2346.

(17) Rodriguez, E. D.; Luo, X.; Mather, P. T. *ACS Appl. Mater. Interfaces* **2011**, *3*, 152−61.

(18) Nji, J.; Li, G. *Smart Mater. Struct.* **2012**, *21*, 025011.

(19) Xie, T.; Rousseau, I. A. *Polymer* **2009**, *50*, 1852−1856.

(20) Luo, X.; Mather, P. T. *Adv. Funct. Mater.* **2010**, *20*, 2649−2656.

(21) Luo, X.; Mather, P. T. *Soft Matter* **2010**, *6*, 2146.

(22) Xiao, X.; Xie, T.; Cheng, Y.-T. *J. Mater. Chem.* **2010**, *20*, 3508.

(23) Kumar, a; Stephenson, L.; Murray, J. *Prog. Org. Coat.* **2006**, *55*, 244−253.

(24) Schmidt, A. M. *Macromol. Rapid Commun.* **2006**, *27*, 1168−1172.

(25) Mohr, R.; Kratz, K.; Weigel, T.; Moneke, M.; Lendlein, A. *Proc. Natl. Acad. Sci. U.S.A.* **2006**, *103*, 3540−3545.